ROBOTICS
AND
MECHATRONICS

ULTRASOUND TISSUE CHARACTERIZATION OF PRM

C. (Catalin) Cernat

MSC ASSIGNMENT

Committee:
prof. dr. ir. S. Stramigioli
S. Das, MSc
prof. dr. ir. C.L. de Korte

July, 2021

035RaM2021
Robotics and Mechatronics
EEMathCS
University of Twente
P.O. Box 217
7500 AE Enschede
The Netherlands

UNIVERSITY OF TWENTE. | TECHMED CENTRE
UNIVERSITY OF TWENTE. | DIGITAL SOCIETY INSTITUTE

Preface

I would like to start by saying that undertaking this master assignment within the RaM department in collaboration with MUSIC group from Radboudumc strengthened my convictions and interests in robotics and image processing. While writing my master thesis I realized that indeed, this is the path I would like to follow as a future career. This is mostly due to the friendly and open environment within the RaM department and MUSIC group and to my supervisors who showed me how beautiful the academic research can be.

I would like to express my special gratitude to my supervisors and committee members S. Das, MSc, Prof. Dr. Ir. C.L. de Korte and Prof. Dr. Ir. S. Stramigioli for all the support offered on my journey of writing this master thesis. Their supportive and positive attitude made my stay within the RaM department and MUSIC group a very pleasant one. Furthermore, I would like to show my sincere appreciation to the secretary, J.M. Boelema - Kaufmann and all the technical staff who were very responsive, helpful and oriented to the student's needs.

Lastly I would like to thank my friends and family who always supported, encouraged and motivated me through my bachelor and master study and while writing this thesis.

Catalin Cernat
Enschede, 29 June 2021

Contents

1 Introduction

The female pelvic floor muscles provide support to the pelvic floor organs and also facilitates the passage of the baby during delivery. This group of muscles is known as the Levator Ani Muscles (LAM). The Puborectalis Muscle (PRM) is one of the muscles in LAM. PRM can stretch up to 250% of their original length during vaginal delivery. This may cause permanent muscle trauma. As a consequence, one fourth to one sixth of all women above the age of sixty suffer from urinary incontinence and pelvic organ prolapse (POP), respectively. This can cause major inconveniences in their daily life. To better understand the mechanisms associated with the pelvic floor muscles, it is necessary to obtain functional and diagnostic information about these muscles.

In order to observe these muscle movements, particularly the PRM, 3D/4D Transperineal Ultrasound (TPUS) is used. While a female candidate voluntarily contracts and relaxes her muscles, the movements of the pelvic muscles are captured in US volumes. Although MRI scans directly generate 3D anatomical visualizations, compared to Ultrasound, they are also more expensive.

1.1 Research goal

The goal of this master assignment is to develop a Quantitative Ultrasound (QUS) tissue characterization technique that can detect pathological changes due to muscle trauma in the PRM. For this purpose, US images of the PRM will be analyzed and through appropriate techniques and models, the state of the muscular tissue will be evaluated.

Ideally the method should be fully automated and provide an accurate classification of the extent of the damage of PRM. To this extent, more specific research questions must be answered thoroughly:

- How are skeletal muscle injuries portrayed in an US image?
- How can the dynamic assessment of a muscle determine the presence of damage?
- What are the main sources that can affect the characterization of the tissue?
- Which image processing techniques can be used to better distinguish between a damaged muscle and an undamaged one?

1.2 Thesis outline

First chapter provides an introduction to the topic alongside the research goal and an outline of the master thesis. Second chapter includes the research article which is the results of the master thesis assignment. The research article is structured as follows: Introduction, Method, Results, Discussion and Conclusion. The conclusion also includes recommendations for future work. Last chapter concludes the thesis by presenting answers to the research questions and an overall conclusion of the results.

Tissue characterization of puborectalis muscle from 3D ultrasound

Catalin Cernat[*†], Shreya Das[†], Frieda van den Noort[*], Claudia Manzini[§] and Chris L. de Korte[†§],
[†]Medical Ultrasound Imaging Center (MUSIC) Radboud University Medical Center, Nijmegen, The Netherlands
[§]Department of Reproductive Medicine and Gynecology University Medical Center, Utrecht, The Netherlands
[*]Electrical Engineering-Robotics and Mechatronics University of Twente, Enschede, The Netherlands
[‡]Physics of Fluids, MIRA University of Twente, Enschede, The Netherlands

***Abstract*—Pelvic floor muscles have the role to prevent pelvic organs' descent. During crowning the puborectalis muscle (PRM), one of the female pelvic floor muscles, can be damaged. This can potentially cause irreversible muscle trauma and even lead to disconnection from its insertion point i.e. avulsion. Ultrasound imaging allows diagnosis of such trauma based on geometric features**

We developed a quantitative ultrasound (QUS) tissue characterization method to obtain information about the state of the tissue of the PRM. The muscle was divided into seven regions of interest (ROIs) and the mean echogenicity, the entropy and the shape parameter of the statistical distribution of gray values were analyzed. This analysis was performed when the muscle was at rest and when it was contracted. We found that, for PRMs with unilateral avulsion compared to undamaged PRMs, the shape parameter was higher ($p < 0.01$), the entropy was lower($p < 0.01$) and mean echogenicity was higher($p = 0.02$). This method might be easily applicable on quantifying PRM damage.

I. Introduction

The female pelvic floor muscles provide support to the pelvic floor organs and also facilitate the passage of the baby during delivery[1]. This group of muscles is known as the Levator Ani Muscles (LAM). The Puborectalis Muscle (PRM) is one of the muscles in LAM. PRM can stretch up to 250% of its original length during vaginal delivery[2]. This may cause permanent muscle trauma and represents a risk factor for later-life pelvic floor dysfunction. After vaginal childbirth, about half of all women present substantial alteration of functional anatomy affecting the puborectalis muscle (PRM) which is currently the best-defined etiological factor in the pathogenesis of pelvic organ prolapse (POP)[3]. As a consequence, one fourth to one sixth of all women above the age of forty suffer from pelvic organ prolapse (POP) and urinary incontinence, respectively[4 5]. This can cause major inconveniences in their daily life. To better understand the mechanisms associated with the pelvic floor muscles and trauma caused to them, functional and diagnostic information about these muscles might be beneficial.

A. Muscle trauma in ultrasound

Microstructural composition of muscle tissue can be assessed indirectly by measuring echogenicity (grayscale with a range 0–255)[6]. As presented by Woodhouse and McNally, strains, tears and laceration are muscle injuries most commonly cause by the overelongation of muscles in the body. These indirect muscle lesions can be visualized with an ultrasound image as areas of altered echogenicity within the muscle. In figure 1 an example of partial tear of muscle fibers of the rectus femoris (located in the upper leg) and a small hematoma are shown.

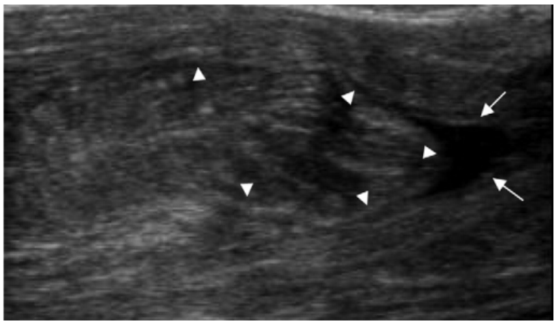

Fig. 1: Rectus femoris showing partial tears(arrowheads) and a small hematoma(arrows)[7]

Recurrent and/or sever muscle injury, on the other hand, can leave behind intramuscular scars which appear as hyperreflective focus or hyperechogenic areas and can alter the functional dynamics of the surrounding muscle[7]. Such an example of a hyperechogenic region due to damage can be seen in figure 2.

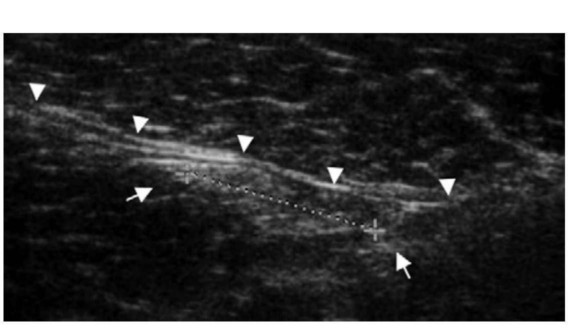

Fig. 2: Scar formation seen after recurrent injury(arrows)[7]

B. Damage and its diagnosis

One of the most common form of macroscopic damage of the LAM is *avulsion*. Avulsion is the dislodgment (disconnection by force) of the PRM from its insertion, the pubic symphysis (PS)[3]. In case of unilateral avulsion, this disconnection of the muscle is from any one side of the bone PS whereas in case of bilateral avulsion, disconnection is from both sides of the PS. This can be diagnosed according to Dietz by palpation or digital assessment of the pelvic floor muscle (PFM) via the vaginal or transanal route. However, this method poses a challenge since the clinician must be trained to diagnose it correctly and the distinction between partial or complete trauma can be hard to detect[8].

The alternative, more reproducible way of diagnosing such trauma is with the aid of ultrasound imaging. 3D/4D Transperineal Ultrasound (TPUS) was first described in 2004[8] to render volumes which then the clinician evaluates by assessing different interslice intervals (2D images within the volume) containing the PRM. Diagnosis of unilateral avulsion is performed by measuring the distance of each end of the insertion point of PRM from the urethra in the 2D images. If this distance is larger than 25mm, then that end of the PRM is considered to be disconnected from its insertion point[8]. Hence the diagnosis is unilateral avulsion.

The aim of this study is to develop a quantitative ultrasound (QUS) tissue characterization method to obtain functional and diagnostic information about the state of the tissue of the PRM. We hypothesized that a change in the state of the tissue within the PRM will result in a change in the statistical distribution of gray values in a B-mode image of the PRM. For this purpose PRMs without avulsion and with unilateral avulsion have been investigated. Furthermore, two distinct scenarios were analyzed: first, when the muscle was at rest and second when the muscle was voluntarily contracted. Based on the findings made by Crema et al., it is expected that the two scenarios will show different results since muscle damages such as tears are more prominent in a contracted muscle. The developed QUS method is then evaluated for statistical significance and using receiver operating characteristic curve (ROC) at various threshold settings.

II. Method

A. Data acquisition

For this work, 3D/4D Transperineal Ultrasound (TPUS) was acquired using Philips X6-1 matrix transducer connected to an EPIQ 7G US machine (Philips Healthcare, Bothell, WA, USA), at the University Medical Centre (UMC), Utrecht, The Netherlands. Data was acquired from the PRM in women without an avulsion (n=8) and in women with unilateral avulsion (n=6). The Medical Research Ethics Committee of UMC Utrecht exempted the project from approval, and all volunteers signed appropriate research consent forms.

All the data from women with undamaged as well as unilateral avulsion of PRM were acquired with the same preset in the US machine. The time gain compensation (TGC) and other settings like filtering or processing were not changed for any acquisition. One volume consists of 352x229x277 pixels(in the X, Y and Z direction respectively) for a total physical volume of 14.78x13.74x9.41 centimeters. In figure 3, a slice of the 3D volume containing the PRM can be seen. The highlighted yellow area represents the PRM. The data were stored in the Digital Imaging and Communications in Medicine (DICOM) format. The volumetric data was acquired at a rate of approximately 1.5 volumes/sec resulting in 22 volumes which span over 15 seconds. During this time window, the women voluntarily contracted their pelvic floor muscles, from rest. Based on the principle of altered echogenicity due to muscle trauma, Crema et al. presented a new approach towards detecting minor muscle injuries. Dynamic ultrasound assessment involves the candidate voluntarily contracting the muscle in order to better expose areas of low echogenicity inside the muscle. These areas could be minor partial tears or minor strains of muscle fibers. These partial tears or minor strains look like ill-defined hypoechogenic areas at rest. Whereas, at contraction these appear as much more prominent areas of low echogenicity. This is analogous to our situation, as the female candidate voluntarily contracts her PRM starting from rest.

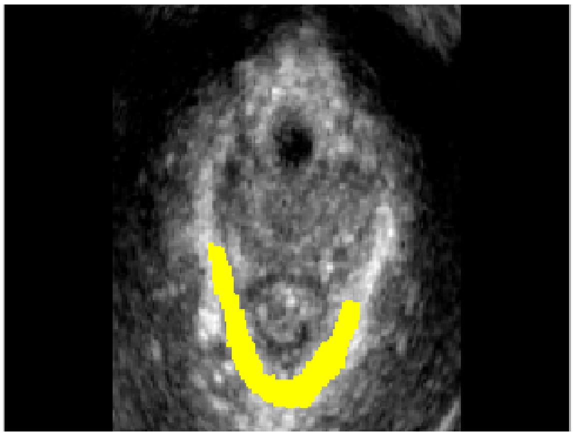

Fig. 3: Slice of a US volume of PRM (top view)

B. Muscle segmentation

The PRM was automatically segmented in the 3D volume using an Active Appearance Model (AAM)[10]. The study showed that automatic segmentation provides volumes similar to manual segmentation of the PRM. For the purpose of this work, the segmented PRM was used. The 3D volume of the segmented muscle can be seen in figure 4.

The segmented volume of the muscle at rest (fig. 4) was tracked over the contraction cycle by calculating intervolumetric displacements for each pair of subsequent volumes using a 3D normalized cross-correlation algorithm[11 12]. The resulting segmentation made it possible to also analyze the PRM in the contracted state. From now on, the 3D segmentation of the PRM, both at rest and contracted, will be referred to as the mask.

Fig. 4: 3D volume of segmented PRM at rest

A PRM with unilateral avulsion presents a disconnection, on one end, from the PS. Meanwhile, an undamaged PRM, without avulsion, has both ends connected to the insertion point on the PS. To better exploit this particularity, the muscle has been further divided into seven regions of interest (ROIs) as shown in figure 5. This has been done by collapsing the 3D mask of the PRM onto a 2D plane which represents the top view of the muscle and was saved as a binary mask. Afterwards, the binary mask was automatically divided into seven ROIs of equal number of points and each ROI has been multiplied, element wise, with the 3D mask. The gray values were extracted by multiplying each ROI with the US volume, slice by slice. When analyzing an undamaged PRM, both regions one and seven were used, while for a PRM with unilateral avulsion, either region one or seven was used. This depends on whether the avulsion is located on the left (region one) or on the right (region seven). This has been done in order to analyze the areas closest to a possible damage, therefore the areas closest to the insertion points.

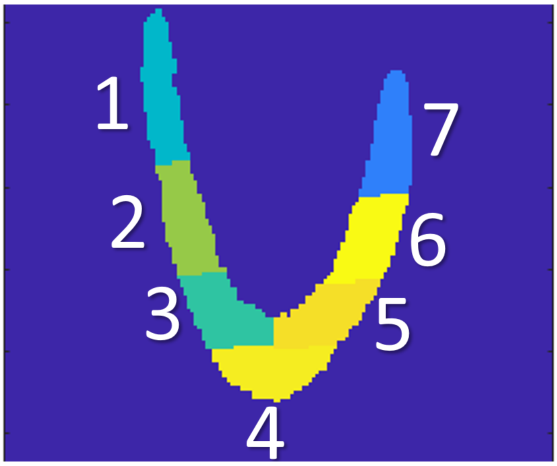

Fig. 5: ROIs of PRM

C. Mean echogenicity

Bellos-Grob showed that structural changes in the puborectalis muscle can be distinguished and analyzed by measuring the mean echogenicity of the muscle (MEP), during and after pregnancy. It was shown that six months postpartrum, MEP was significantly ($p < 0.001$) lower than the values during pregnancy. Therefore it is expected that structural changes due to muscle trauma can also be analyzed using mean echogenicity. Mean echogenicity can be calculated by summing the grey values of the pixels in each ROI and dividing the result by the number of pixels in that ROI.

D. Shannon's entropy

Shannon's entropy is a widely used QUS technique for ultrasound tissue characterization which measures the signal uncertainty or level of information. Chen et al. investigated the clinical value of Shannon's entropy in grading different stages of hepatic steatosis. The results were compared to a deep learning VGG-16 model. It was shown that Shannon's entropy outperformed VGG-16 in identifying candidates with moderate or severe hepatic steatosis. Furthermore, Chen et al. showed that when compared to a conventional statistical parametric based on Nakagami distribution, Shannon's entropy outperformed it with a 10% higher area under the receiver operating characteristic (ROC) curve. For a given ROI, Shannon's entropy can be calculated as[13]:

$$\mathrm{H_C} = -\sum_{i=1}^{n} w\left(y_i\right) \log_2 \left[w\left(y_i\right)\right] \tag{1}$$

where $w\left(y_i\right)$ represents the probability value obtained from the normalized histogram counts, n is the number of bins in the histogram and y_i is the discrete random variable of the backscattered echo intensity.

It is expected that a change in the structure of the PRM will result in a change in the entropy, therefore change in the level of information that an area within the PRM may contain.

E. Statistical distribution of gray values

As mentioned by Girardi, tissue microstructure information can be found in the envelope of the backscattered ultrasonic echo. The radio-frequency (RF) signals backscattered from tissue are dependent on the shape, size and density of the scatterers inside the tissue[15]. According to statistics of ultrasound echoes measured from biological tissues, the envelope can be classified as pre-Rayleigh, Rayleigh, and post-Rayleigh distributions. All these three types of distributions can be modeled by Nakagami distribution. The probability distribution of the Nakagami model is given by[16]:

$$p_A(A \mid m, \Omega) = \frac{2m^m A^{2m-1}}{\Gamma(m)\Omega^m} * \exp\left(\frac{-mA^2}{\Omega}\right) * U(A) \tag{2}$$

where $U(\cdot)$ is the unit step function, $\Gamma(\cdot)$ is the gamma function, m is the Nakagami shape(or spread) parameter and Ω is the scaling factor.

If the envelope follows a Nakagami distribution, then the intensity follows a gamma distribution[17] and the probability density function (PDF) is given by:

$$P_{\text{Gamma}}\left(I \mid \alpha, \beta\right)=\frac{\beta^{\alpha}}{\Gamma(\alpha)} I^{\alpha-1} e^{-\beta I} \tag{3}$$

where α is the shape parameter, and β is the rate parameter.

The shape parameter of the Gamma distribution resulted from the pixels distribution within each ROI of the B-MODE image of the PRM. It was determined using a maximum likelihood estimator. It is expected that a change in the tissue microstructure will be reflected in a change of the pixel distribution in each ROI, resulting in a change in the shape parameter as well.

F. Analysis procedure

The mean echogenicity, entropy and the shape parameter values of the Gamma distribution were computed for each ROI. Since the sample size was small, the Wilcoxon Rank Sum Test was used to determine whether the computed values could be described by distributions with equal medians implying that, the proposed parameters cannot be used to distinguish between a damaged or an undamaged PRM. Furthermore, for each parameter, the receiver operating characteristic (ROC) curve was computed and the area under the curve (AUC) was calculated in order to compare the diagnostic ability of a classifier using each of the three parameters described above. The ROC curve is created by plotting the true positive rate (TPR) against the false positive rate (FPR) at various threshold settings. Since the amount of data points in the graph is equal to the dataset, a polynomial curve was fit on top of the original graph [18]. This has been done in order to the an idea of the trend presented by the points.

III. Results

Figure 6 presents the results for the mean echogenicity, entropy and shape parameter values as boxplots in a side by side comparison for the undamaged and damaged PRM both at rest and at contraction. ”On each box, the central mark indicates the median, and the bottom and top edges of the box indicate the 25th and 75th percentiles, respectively. The whiskers extend to the most extreme data points not considered outliers. The outliers are plotted individually using the $'+'$ symbol.” [19]

Figure 7 shows the ROC curves for the same scenarios. Here the blue dots represent discrete transition points while the red line represents the approximated curve based on those points.

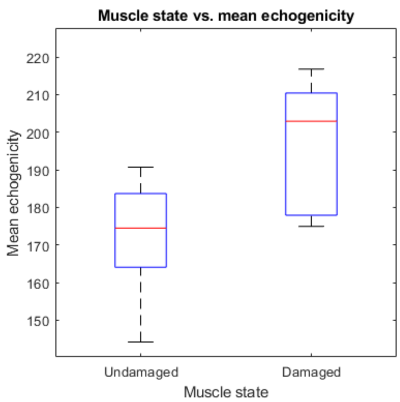

(a) Mean echogenicity at rest

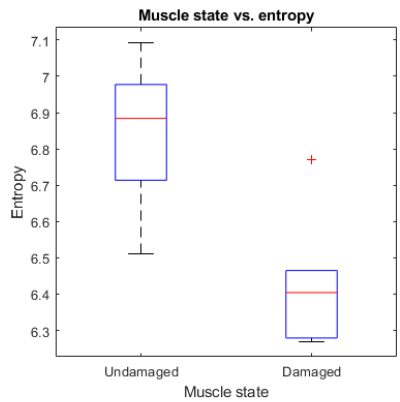

(b) Entropy at rest

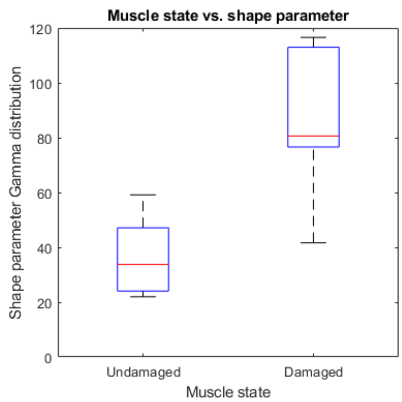

(c) Shape parameter at rest

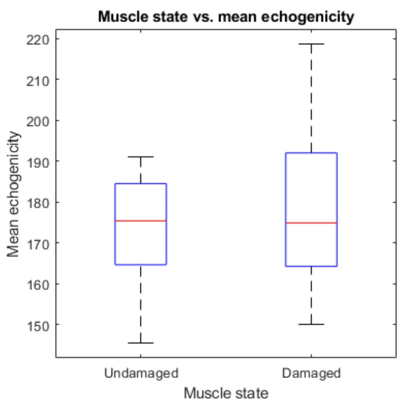

(d) Mean echogenicity at contraction

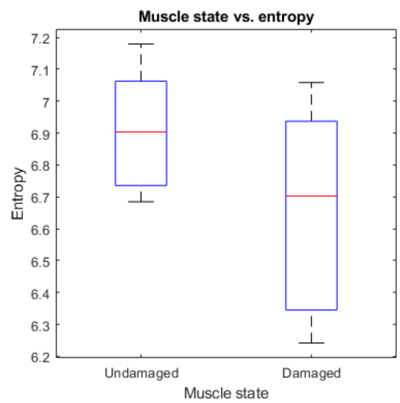

(e) Entropy at contraction

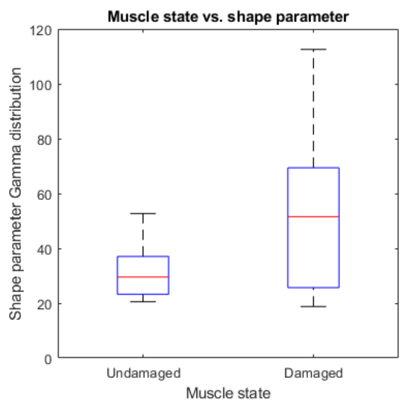

(f) Shape parameter at contraction

Fig. 6: Mean echogenicity, entropy and shape parameter value for PRM without avulsion and with unilateral avulsion, at rest (top row) and contracted (bottom row)

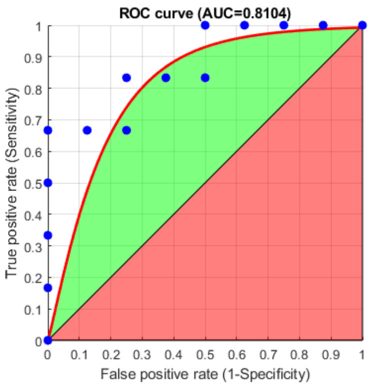

(a) ROC mean echogenicity at rest

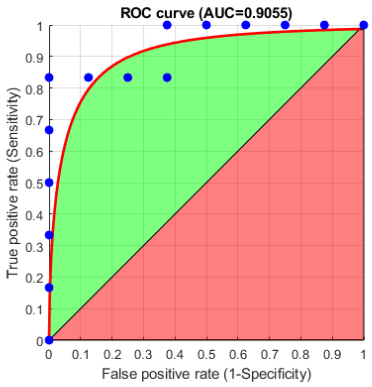

(b) ROC entropy at rest

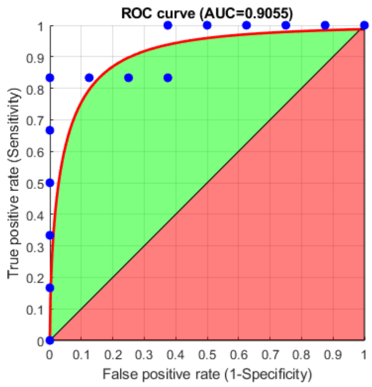

(c) ROC shape parameter at rest

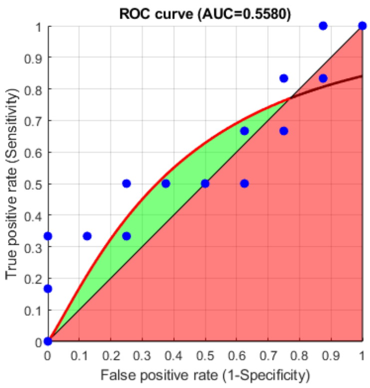

(d) ROC mean echogenicity at contraction

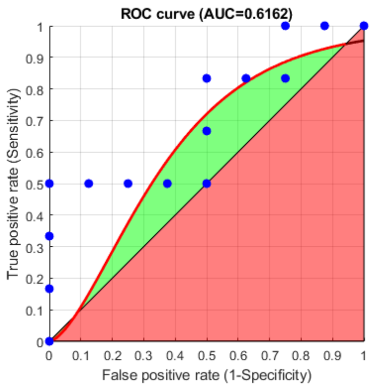

(e) ROC entropy at contraction

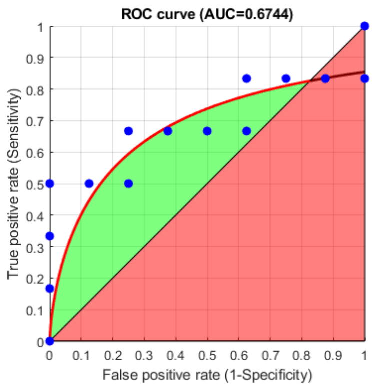

(f) ROC shape parameter at contraction

Fig. 7: ROC curves for mean echogenicity, entropy and shape parameter when PRMs were at rest (top row) and when PRMs were at contraction (bottom row). Here the blue dots represent discrete transition points, while the red line is the approximated (fitted) curve based on those points

A. *Mean echogenicity*

When PRMs were at rest, the mean echogenicity showed an increase (p-value=0.02) for PRMs with unilateral avulsion compared to PRMs without avulsion. The distance between the estimated means of the two classes was found to be 25.22 and the AUC for the fitted curve of 0.81. For the case when PRMs were at contraction, the mean echogenicity showed an increase (p-value=0.28) for PRMs with unilateral avulsion compared to PRMs without avulsion. However this is not visible in figure 6d due to the fact that the boxplots focus on the median rather than mean values. This is desirable since for small datasets, median values give a much accurate representation. The distance between the estimated means of the two classes was found to be 5.93 and the AUC for the fitted curve was 0.55.

B. *Entropy*

When PRMs were at rest, the entropy showed a decrease ($p - value < 0.01$) for PRMs with unilateral avulsion compared to PRMs without avulsion. The distance between the estimated means of the two classes was found to be 0.412 and the AUC for the fitted curve was 0.91. For the case when PRMs were at contraction, the entropy showed a decrease (p-value=0.22) for PRMs with unilateral avulsion compared to PRMs without avulsion. The distance between the estimated means of the two classes was found to be 0.24 and the AUC for the fitted curve was 0.61.

C. *Shape parameter of Gamma distribution*

When PRMs were at rest, the shape parameter value showed an increase ($p - value < 0.01$) for PRMs with unilateral avulsion compared to PRMs without avulsion. The distance between the estimated means of the two classes was found to be 48.44 and the AUC for the fitted curve was 0.91. For the case when PRMs were at contraction, the shape parameter showed an increase (p-value=0.28) for PRMs with unilateral avulsion compared to PRMs without avulsion. The distance between the estimated means of the two classes was found to be 23.3 and the AUC for the fitted curve was 0.67.

D. *Summarized results*

The summarized results for the distance between the means, the statistical significance and the AUC for the fitted curve and

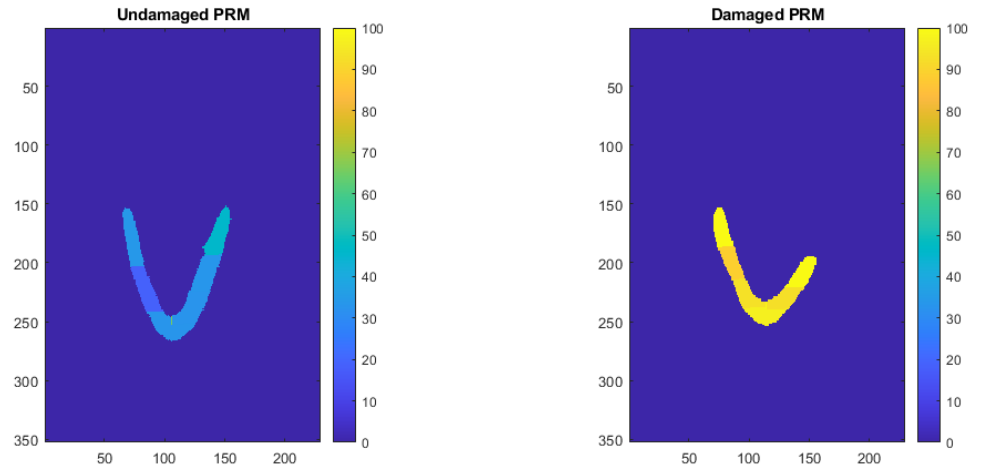

(a) Undamaged PRM with all pixels in each ROI replaced by the shape parameter value

(b) Damaged PRM with all pixels in each ROI replaced by the shape parameter value

Fig. 8: Visual representation of the shape parameter change for an undamaged and damaged PRM

the exact curve for each parameter can be found in table I for PRMs at rest and in table II for PRMs at contraction.

TABLE I: Summarized results for the three parameters with PRMs at rest

	AT REST		
	Mean echogenicity	Entropy	Shape parameter
Distance between means	25.22	0.41	48.44
Statistical significance (p-value)	0.02	< 0.01	< 0.01
AUC fitted curve	0.81	0.91	0.91
AUC exact curve	0.87	0.93	0.93

TABLE II: Summarized results for the three parameters with PRMs at contraction

	AT CONTRACTION		
	Mean echogenicity	Entropy	Shape parameter
Distance between means	5.93	0.24	23.3
Statistical significance (p-value)	0.66	0.22	0.28
AUC fitted curve	0.55	0.61	0.67
AUC exact value	0.58	0.70	0.68

IV. Discussion

In this paper we described a method for quantitative ultrasound analysis of the damaged PRM to distinguish the avulsion from the non-avulsion side. The principal finding of the study is that the echogenicity parameters investigated in this study for the avulsion side are different from the non-avulsion side when the PRM is at rest. In women without avulsion, the echogenicity based parameters of the two sides of the PRM are similar. During contraction, the difference between avulsion and non-avulsion side is not present anymore. We noticed that at rest, the statistical significance and the AUC (< 0.01 and 0.91 respectively) for entropy and shape parameter are similar. At contraction, all parameters performed worse in classifying the damaged PRMs from the undamaged ones. This could hint that formation of scar tissue is predominant since according to Crema et al. only tears are better distinguishable when a muscle contracts. However, since the parameters analyzed cannot discern between tears and scar tissue this has to be further investigated.

Furthermore, by assessing each ROI within the PRM the value of the shape parameter, images were created which can provide visual aid to the clinician in diagnosing all sections of the PRM, not only the ones closest to the insertion point. This way, information regarding the locality of the damage within the PRM were brought to surface. Such an example can be seen in figures 8a and 8b. Here the blue color corresponding to low values of the shape parameter indicates areas of undamaged tissue. Yellow color, corresponding to high values of the shape parameter indicates areas of damaged tissue.

A. Limitations and shortcomings

On main limitation and two shortcomings of the method have been identified. The limitation is that the size of the dataset (n=14) was small which resulted in the use of a non parametric test for evaluation. This limits the techniques that could be used to rather conventional ones as opposed to more modern, machine learning/deep learning oriented ones.

The first shortcoming was the use of the B-MODE images instead of RF data. It makes the application of this method machine dependent. Although for this work the data acquisition has been performed by the same clinician, using the same machine and settings, this criterion cannot always be ensured. Further investigation on different data formats and machines is necessary to ensure consistency.

The second shortcoming is that although the methods proposed can distinguish between PRMs with and without avulsion relative to each other, no conclusion can be drawn regarding the type of damage/trauma each muscle had suffered. The increase in the mean echogenicity of the PRMs with unilateral avulsion, at rest, might indicate scar tissue formation, although this conclusion cannot be drawn from this measurement alone.

Furthermore, although Woodhouse and McNally indicates that High-frequency linear array probes, $> 7MHz$ and preferably $> 10MHz$, are required to adequately image muscle, a $1 - 6MHz$ matrix probe has been used. This is due to the fact that increased depth resolution (achieved through higher ultrasound frequencies) comes at the cost of decreased ability to image deep structures[7]. Therefore it was crucial that depth penetration was ensured such that the PRM can be captured completely.

B. Future directions

The results obtained in this paper show the potential of quantitative echography to identify PRM avulsion. The different parameters could serve as input (a so called feature) for more specialized machine learning algorithms such as neural networks. However, it is crucial for such applications that the dataset is enlarged to a level which allows training and testing of such algorithms.

On the other hand, a deep learning approach could be used for both feature detection and classification. An entire segmented PRM could be fed to a deep neural network (DNN) or convolutional neural network (CNN) which could potentially classify both the state of the muscle (damaged and undamaged) as well as the type of trauma that the muscle could have suffered. For this scenario, only the database of segmented PRMs has to be increased.

V. Conclusion

In this study, we used mean echogenicity, Shannon's entropy and shape parameter value based on log-compressed B-MODE images for assessing the state of the puborectalis muscle (PRM) in two scenarios: at rest and contracted. The results demonstrate that the shape parameter of the first order statistics of the speckle (gray value distribution) is the strongest parameter to distinguish intact and damaged PRM resulting in the highest AUC. The entropy has slightly less performance. Analysis of the muscle at contraction has decreased performance with respect to analysis at rest. This supports the hypothesis that a change in the state of the tissue will result in a change in the statistical distribution of gray values in a B-mode image of the PRM.

References

[1] J.O.L. DeLancey. *Pelvic Floor Anatomy and Pathology*. Elsevier Inc, University of Michigan, Ann Arbor, MI, United States of America, 2016.

[2] K Svabík, KL Shek, and HP Dietz. How much does the levator hiatus have to stretch during childbirth? *BJOG: An International Journal of Obstetrics & Gynaecology*, 116(12):1657–1662, 2009. doi: https://doi.org/10.1111/j.1471-0528.2009.02321.x. URL https://obgyn.onlinelibrary.wiley.com/doi/abs/10.1111/j.1471-0528.2009.02321.x.

[3] Hans Peter Dietz. Pelvic floor trauma in childbirth. *Australian and New Zealand Journal of Obstetrics and Gynaecology*, 53(3):220–230, 2013. doi: https://doi.org/10.1111/ajo.12059. URL https://obgyn.onlinelibrary.wiley.com/doi/abs/10.1111/ajo.12059.

[4] Dina Bedretdinova, Xavier Fritel, Henri Panjo, and Virginie Ringa. Prevalence of female urinary incontinence in the general population according to different definitions and study designs. *European Urology*, 69(2):256–264, 2016. ISSN 0302-2838. doi: https://doi.org/10.1016/j.eururo.2015.07.043. URL https://www.sciencedirect.com/science/article/pii/S0302283815007022.

[5] Alexis A. Dieter, Maggie F. Wilkins, and Jennifer M. Wu. Epidemiological trends and future care needs for pelvic floor disorders. *Current Opinion in Obstetrics & Gynecology*, 27(5):380–384, 2015. doi: 10.1097/gco.0000000000000200.

[6] Anique Theodora Maria Bellos-Grob. *Structural and functional ultrasound imaging of the pelvic floor during pregnancy and postpartum*. PhD thesis, Utrecht University, December 2016.

[7] Joe B. Woodhouse and Eugene G. McNally. Ultrasound of skeletal muscle injury: An update. *Seminars in Ultrasound, CT and MRI*, 32(2):91–100, 2011. ISSN 0887-2171. doi: https://doi.org/10.1053/j.sult.2010.12.002. URL https://www.sciencedirect.com/science/article/pii/S0887217110001265. Musculoskeletal Ultrasonography.

[8] Hans Peter Dietz. Pelvic floor muscle trauma. *Expert Review of Obstetrics & Gynecology*, 5(4):479–492, 2010. doi: 10.1586/eog.10.28. URL https://doi.org/10.1586/eog.10.28.

[9] Michel Crema, Andre Yamada, Ali Guermazi, Frank Roemer, and Abdalla Skaf. Imaging techniques for muscle injury in sports medicine and clinical relevance. *Current reviews in musculoskeletal medicine*, 8, 02 2015. doi: 10.1007/s12178-015-9260-4.

[10] F. van den Noort, A. T. M. Grob, C. H. Slump, C. H. van der Vaart, and M. van Stralen. Automatic segmentation of puborectalis muscle on three-dimensional transperineal ultrasound. *Ultrasound in Obstetrics & Gynecology*, 52(1):97–102, 2018. doi: https://doi.org/10.1002/uog.18927. URL https://obgyn.onlinelibrary.wiley.com/doi/abs/10.1002/uog.18927.

[11] K Gijsbertse, A M J Sprengers, M M Nillesen, H H G Hansen, R G P Lopata, N Verdonschot, and C L de Korte. Three-dimensional ultrasound strain imaging of skeletal muscles. *Physics in Medicine and Biology*, 62(2):596–611, dec 2016. doi: 10.1088/1361-6560/aa5077. URL https://doi.org/10.1088/1361-6560/aa5077.

[12] Gijs A G M Hendriks, Branislav Holländer, Jan Menssen, Andy Milkowski, Hendrik H G Hansen, and Chris L de Korte. Automated 3d ultrasound elastography of the breast: a phantom validation study. *Physics in Medicine and Biology*, 61(7):2665–2679, mar 2016. doi: 10.1088/0031-9155/61/7/2665. URL https://doi.org/10.1088/0031-9155/61/7/2665.

[13] Jheng-Ru Chen, Yi-Ping Chao, Yu-Wei Tsai, Hsien-Jung Chan, Yung-Liang Wan, Dar-In Tai, and Po-Hsiang Tsui. Clinical value of information entropy compared with deep learning for ultrasound grading of hepatic steatosis. *Entropy*, 22(9), 2020. ISSN 1099-4300. doi: 10.3390/e22091006. URL https://www.mdpi.com/1099-4300/22/9/1006.

[14] Arianna Girardi Girardi, A. *Ultrasonic Tissue Characterization inthe Puborectal Muscle*. PhD thesis, University of Twente, 2018.

[15] Po-Hsiang Tsui, Cheng-Wei Hsu, Ming-Chih Ho, Yung-Sheng Chen, Jen-Jen Lin, Leo Chien, and Chin-Chou Chu. Three-dimensional ultrasonic nakagami imaging for tissue characterization. *Physics in medicine and biology*, 55:5849–66, 10 2010. doi: 10.1088/0031-9155/55/19/015.

[16] Mohana Shankar P. A general statistical model for ultrasonic backscattering from tissues. *IEEE Trans Ultrason Ferroelectr Freq Control*, 47(3):727–36, 2000. doi: 10.1109/58.842062.

[17] Siddhartha Sikdar, Guoqing Diao, Diego Turo, Christopher J. Stanley, Abhinav Sharma, Amy Chambliss, Loretta Laughrey, April Aralar, and Diane L. Damiano. Quantification of muscle tissue properties by modeling the statistics of ultrasound image intensities using a mixture of gamma distributions in children with and without cerebral palsy. *Journal of Ultrasound in Medicine*, 37(9):2157–2169, 2018. doi: https://doi.org/10.1002/jum.14566. URL https://onlinelibrary.wiley.com/doi/abs/10.1002/jum.14566.

[18] Giuseppe Cardillo. *ROC curve (https://github.com/dnafinder/roc)*. GitHub, 2021.

[19] MATLAB. *(R2021a)*. The MathWorks Inc., Natick, Massachusetts, 2021.

2 Conclusion

The results presented in this work demonstrate that the shape parameter of the first order statistics of the speckle has the strongest statistical significance as well as highest AUC. Throughout the research conducted, the research questions proposed in the first chapter have been answered thoroughly.

How are skeletal muscle injuries portrayed in an US image?

Based on the US image, muscle injuries can be categorized as follows: injuries that produce low echogenicity hypogechogenic or areas inside the US image of the muscle and injuries that produce hyperechogenic areas. Injuries that produce hypogechogenic areas are tears, lacerations and hematomas. Formation of scar tissue after repeated and/or severe muscle trauma, however, can be seen as areas or hyperechogenicity within a US image of the muscle.

It was expected that through image processing, this difference can be evaluated for PRMs with avulsion and PRMs without avulsion. It has been shown through the analysis that the mean echogenicity, entropy and shape parameter values differ for undamaged PRMs and damaged PRMs, both at contraction and at rest.

How can the dynamic assessment of a muscle determine the presence of damage?

Literature review revealed that dynamic ultrasound assessment involves voluntarily contraction of the muscle by the candidate in order to better expose areas of low echogenicity in the muscle image. These areas could be minor partial tears or minor strains of muscle fibers which, at rest, look like ill defined hypoechogenic areas. It has been shown through the analysis that the mean echogenicity, entropy and shape parameter values differ for PRMs at rest and PRMs at contraction. This difference has been noticed mostly for the PRMs with avulsion.

What are the main sources that can affect the characterization of the tissue?

For the purpose of this assignment, B-mode images have been analyzed. Through literature review, it has been found that this introduces machine dependency. This dependency is variable because not all US machines compress and post process the RF data the same way. Fortunately for this assignment, the same machine has been used for all data acquisition.

Furthermore, the same settings (such as Time Gain Compensation (TGC), filtering etc) have been preserved while acquiring 3D volumes of the pelvic floor. This enabled analysis for PRMs of different women without the need for additional corrections, therefore simplifying the process.

Which image processing techniques can be used to better distinguish between a damaged muscle and an undamaged one?

Through literature review it has been found that statistical distribution of the gray values within a B-mode image can be analyzed. The distribution can be modeled using the Gamma distribution. Furthermore, entropy and mean echogenicity values can be calculated for any given ROI in the muscle. Those parameters have been used in earlier studies to characterize different tissues and it is expected that they could be used to characterize the PRM as well.

It has been shown through the analysis that the mean echogenicity, entropy and shape parameter values can be used to distinguish between a damaged and undamaged PRMs. Statistical analysis revealed that the differences found in PRMs with avulsion compared to the ones without avulsion is statistically significant, therefore the results obtained are not random.

A Appendix 1

A.1 Optimal division of the PRM into multiple subdivisions of the segmentation/ROIs

Division of the PRM into multiple subdivisions of the segmentation/ROIs has been done in order to enable the analysis of the areas closest to the site of the avulsion. It is known that when the PRM suffers a trauma, it can be a unilateral avulsion or a bilateral avulsion. Therefore, the most damaged areas are represented by the muscle tissue closest to the insertion point.To this extent, analysis of those subdivisions of the segmentation/ROIs is preferred over analysis of the entire segmentation of the PRM.

To assess the quality of the subdivisions of the PRM, the distance between the means of the shape parameter for the two categories(with and without avulsion) and the length of the interval for the estimated mean with 95% confidence have been used. A higher difference between the means represents a better discrimination between damaged and undamaged PRMs. Lower interval length of the estimated mean results in a better approximation of the mean.

Due to the relatively low number of included women, the Student's t distribution with n-1 degrees of freedom was used to determine the confidence interval of the mean shape parameter. The results of the estimated mean vs. number of subdivisions of the PRM can be seen in figure A.1. From this figure alone we can conclude that the optimal number of subdivisions of the PRM is eight.

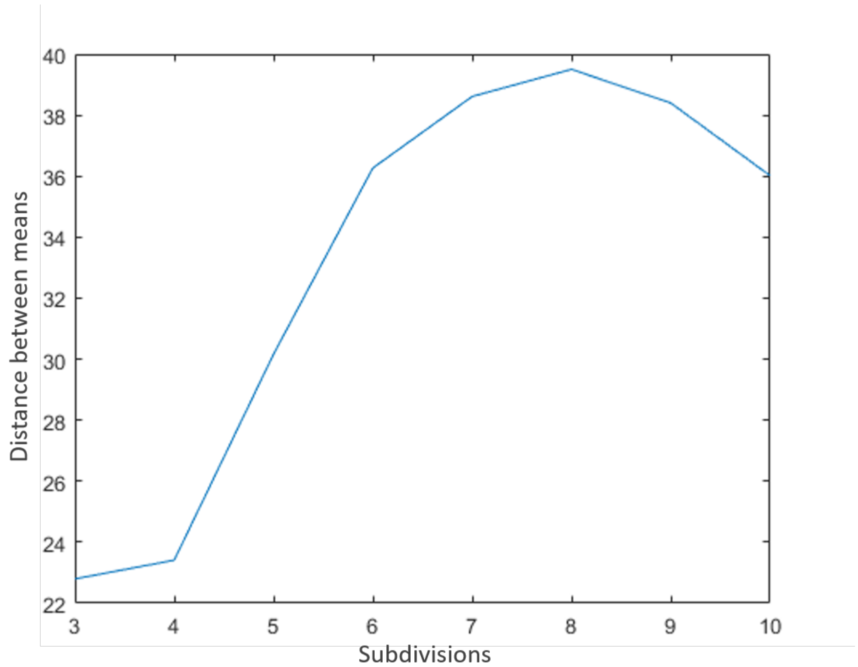

Figure A.1: Mean distance between the two categories of PRM (with and without avulsion) vs. the number of subdivisions

In figure A.2 the length of the interval of the estimated mean with 95% confidence can be seen plotted against the number of subdivisions. From this figure alone, we can conclude that higher number of subdivisions leads to higher the interval length. Higher interval length means that it is harder to accurately approximate the mean.

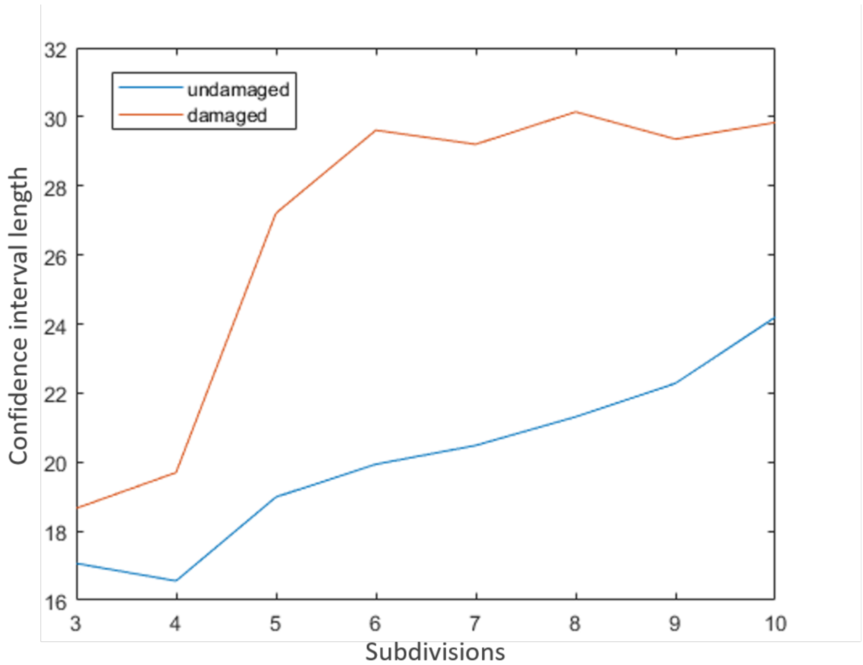

Figure A.2: Interval length for damaged and undamaged PRMs

However, the optimal number of subdivision of the PRM can be achieved by looking at both figures A.1 and A.2 together. To do so, the mean interval length has been calculated for both the damaged and undamaged PRMs. The distance between the means of the shape parameter has been divided by the mean interval length in order to identify the optimal division of the PRM. The results can be seen in figure A.3 and the optimal number of divisions of the PRM was found to be seven.

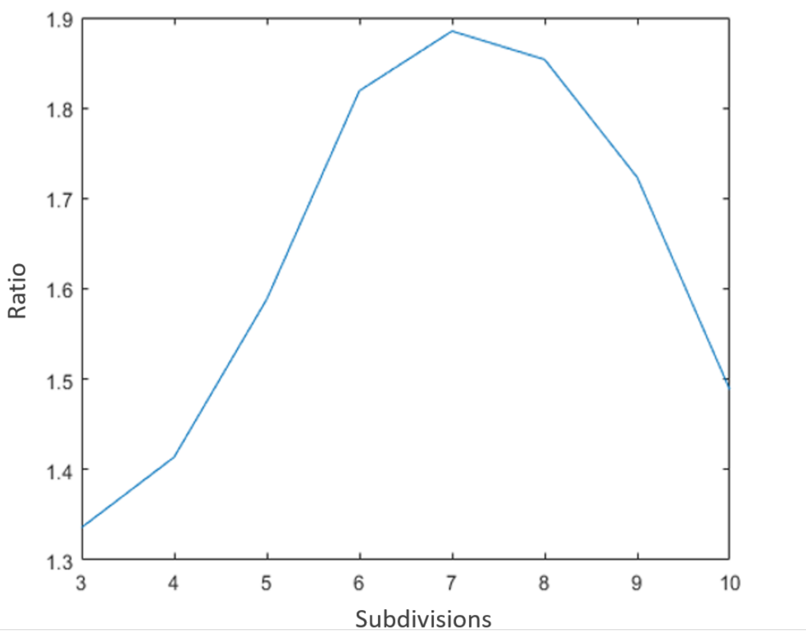

Figure A.3: Ratio vs. number of subdivisions

A.2 Shape parameter mapping for all PRMs

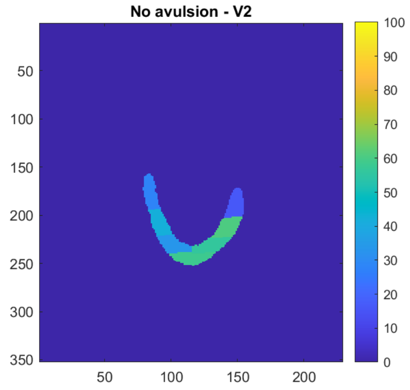

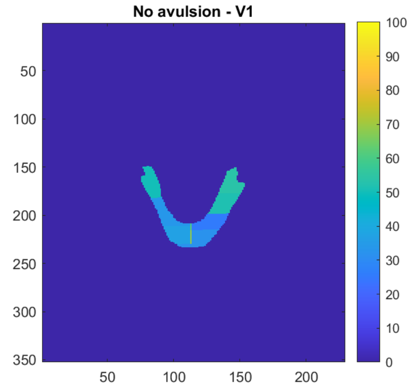

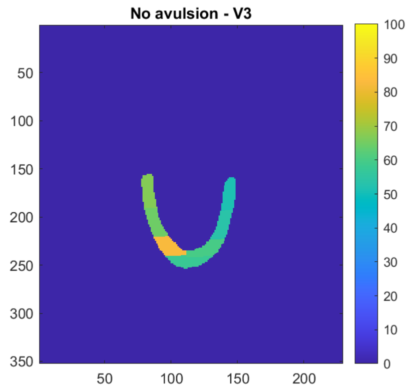

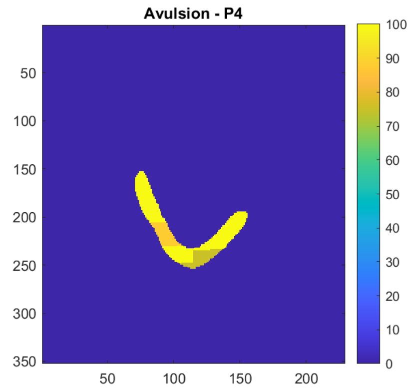

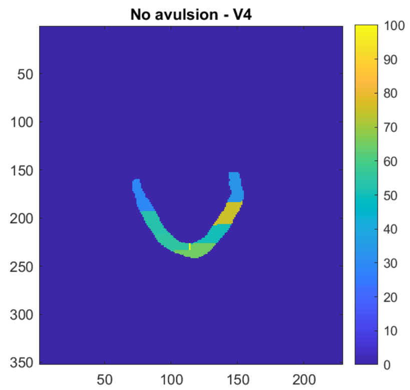

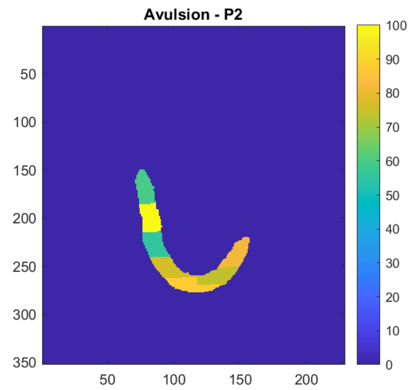

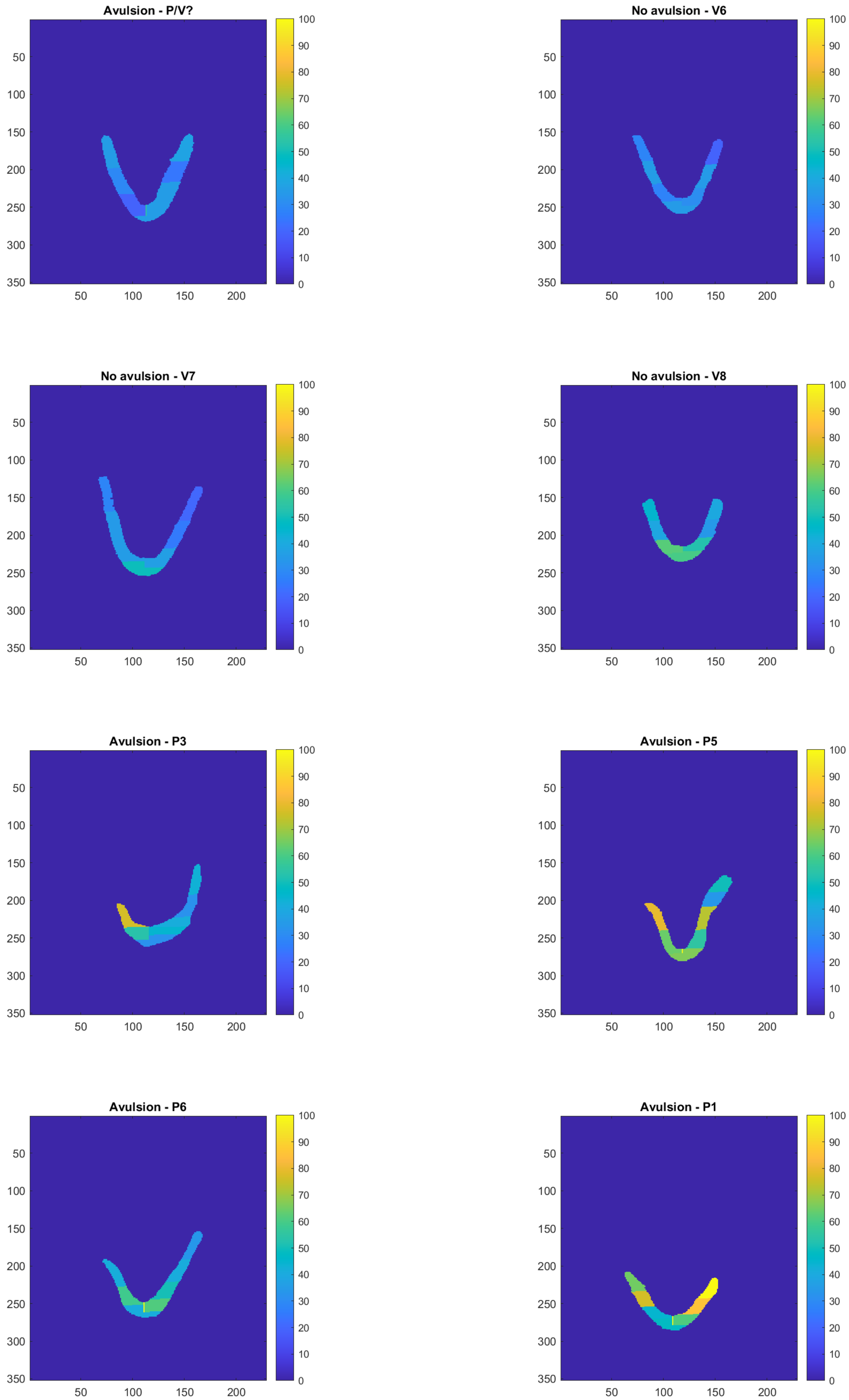
Avulsion - P/V?
No avulsion - V6
No avulsion - V7
No avulsion - V8
Avulsion - P3
Avulsion - P5
Avulsion - P6
Avulsion - P1